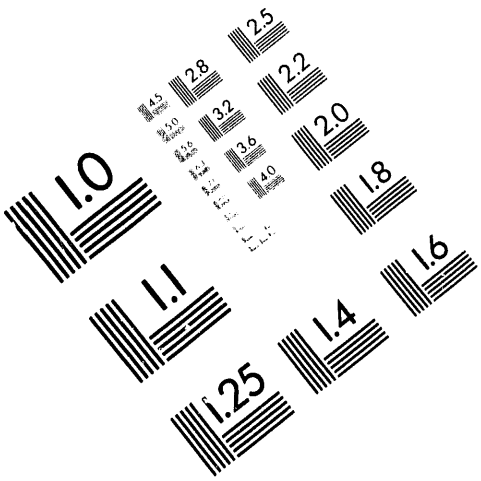

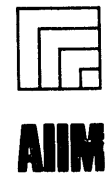

Association for Information and Image Management
1100 Wayne Avenue, Suite 1100
Silver Spring, Maryland 20910
301/587-8202

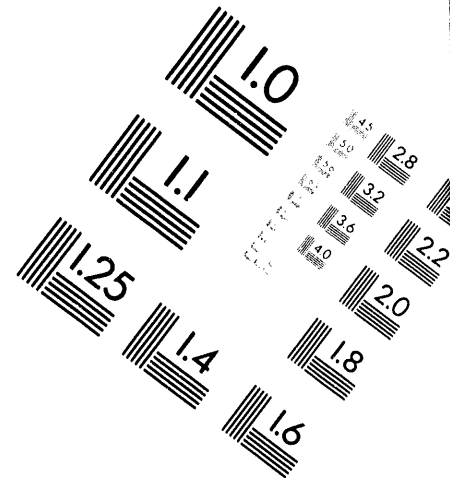

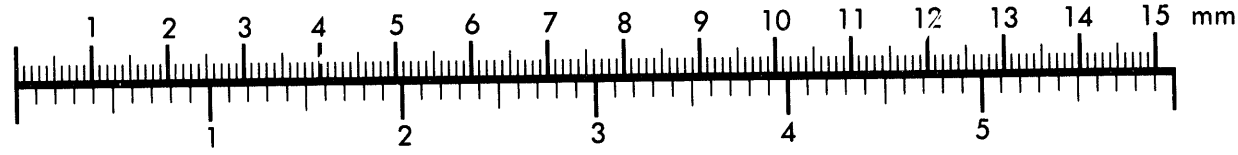

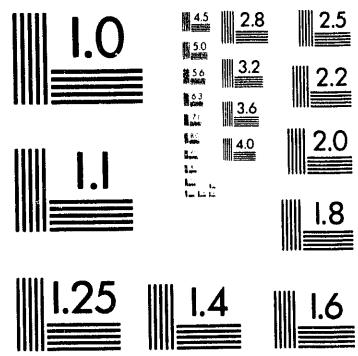

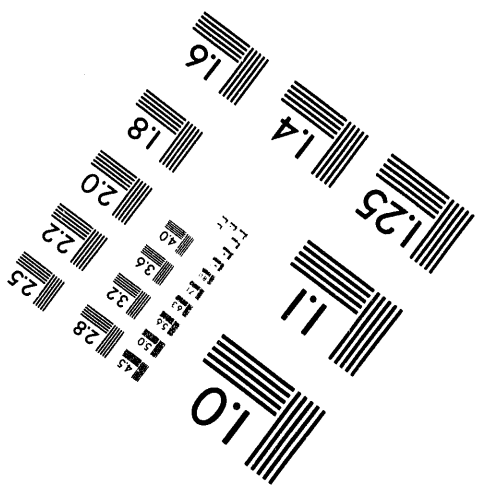

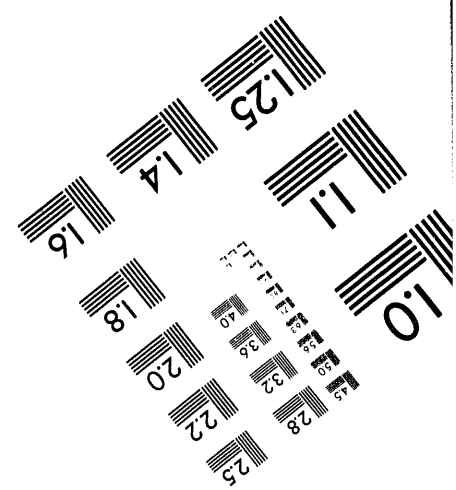

1 of 1

ORNL/TM -12776
ISPO-367

COMPUTING APPLICATIONS DIVISION

MULTIDETECTOR CALIBRATION FOR MASS SPECTROMETERS

C. K. Bayne, D. L. Donohue,[1] R. Fiedler[1]

[1]IAEA, Safeguards Analytical Laboratory, Seibersdorf, Austria.

Date Published: June 1994

UNITED STATES PROGRAM FOR TECHNICAL ASSISTANCE TO IAEA SAFEGUARDS

POTAS DEPARTMENT OF STATE
DEPARTMENT OF ENERGY
ARMS CONTROL AND DISARMAMENT AGENCY
NUCLEAR REGULATORY COMMISSION

This work was sponsored by the U.S. Program for Technical Assistance to IAEA Safeguards (POTAS) under Task D.66: "Consultants - Statistics/Programming for Implementation of a Quality Control System at the Safeguards Analytical Laboratory (SAL)."

Prepared by the
OAK RIDGE NATIONAL LABORATORY
Oak Ridge, Tennessee 37831
managed by
MARTIN MARIETTA ENERGY SYSTEMS, INC.
for the
U.S. DEPARTMENT OF ENERGY
under contract DE-AC05-84OR21400

CONTENTS

LIST OF TABLES

LIST OF FIGURES

ACKNOWLEDGMENTS

This work was supported by the U.S. Program for Technical Assistance to the International Atomic Energy Agency (IAEA) Safeguards (POTAS) under Task D.66. Oak Ridge National Laboratory (ORNL) is managed by Martin Marietta Energy Systems, Inc., under contract DE-AC05-84OR21400 with the U.S. Department of Energy. We also wish to thank Stein Deron of IAEA's Safeguards Analytical Laboratory, David H. Smith of ORNL's Chemical and Analytical Science Division, and Max Morris of ORNL's Engineering Physics and Mathematics Division for their helpful comments and review of this manuscript. Production of this manuscript was only possible with the help of Ms. Paulette F. Rice of the Computing Applications Division and Ms. Catherine H. Shappert of Information Management Services.

EXECUTIVE SUMMARY

The International Atomic Energy Agency's Safeguards Analytical Laboratory has performed calibration experiments to measure the different efficiencies among multi-Faraday detectors for a Finnigan-MAT 261 mass spectrometer. Two types of calibration experiments were performed: (1) peak-shift experiments and (2) peak-jump experiments. For peak-shift experiments, the ion intensities were measured for all isotopes of an element in different Faraday detectors. Repeated measurements were made by shifting the isotopes to various Faraday detectors. Two different peak-shifting schemes were used to measure plutonium (UK Pu5/92138) samples. For peak-jump experiments, ion intensities were measured in a reference Faraday detector for a single isotope and compared with those measured in the other Faraday detectors. Repeated measurements were made by switching back-and-forth between the reference Faraday detector and a selected Faraday detector. This switching procedure is repeated for all Faraday detectors. Peak-jump experiments were performed with replicate measurements of ^{239}Pu, ^{187}Re, and ^{238}U.

Detector efficiency factors were estimated for both peak-jump and peak-shift experiments using a flexible calibration model to statistically analyze both types of multidetector calibration experiments. Calculated detector efficiency factors were shown to depend on both the material analyzed and the experimental conditions. A single detector efficiency factor is not recommended for each detector that would be used to correct routine sample analyses. An alternative three-run peak-shift sample analysis should be considered. A statistical analysis of the data from this peak-shift experiment can adjust the isotopic ratio estimates for detector differences due to each sample analysis.

Key words: Multidetector calibration, Peak-jump experiments, Peak-shift experiments, Detector efficiency factors.

1. INTRODUCTION

Single detector systems for thermal ionization mass spectrometers sequentially measure the ion intensity of each isotope. All ion-intensity measurements are made with the same detector, but a correction is needed because there is a time lag between different mass measurements. The arrival of multidetector systems for mass spectrometers eliminated the need for time-lag corrections because all ion-intensity measurements are made simultaneously with an array of detectors. The amplification systems are adjusted electronically for any gain differences among the detectors. But, ion-intensity measurements may not be equivalent in different detectors because detectors may vary with respect to their geometry, construction, component materials, etc.

Fiedler and Donohue [1] developed a method to estimate the detector efficiency factors (DEFs) by shifting the mass spectrum one or two mass units on each side of its normal position. Fiedler and Donohue's method can estimate the DEFs, but it has some drawbacks: (1) the "true values" of the isotopic ratios are required for estimating DEFs, (2) no straightforward method exists which can estimate error limits on the calculated DEFs, and (3) no standard statistical method is available to test the equality of DEFs or if they are significantly different than 1. In addition, ion-intensity measurements are assumed to decrease linearly within different runs. Investigation of this assumption suggests that a more complex decay function may be required to approximate decreasing ion intensities.

This reports attempts to correct these drawbacks by modeling the ion-intensity measurements with a multiplicative function of experimental factors. This calibration model includes effects caused by mass variations, run variations, and detector variations. The calibration model is assumed to be intrinsically linear so that the logarithms (base e) of the ion-intensity measurements can be used to estimate model parameters. By using this modeling approach, estimating DEFs, testing for the significance of their differences and calculating error limits can be done by standard linear regression methodology [2,3]. In addition, the accuracy of the calibration model fitted to experimental data is examined by comparing estimated isotopic ratio values with their reference values and by inspecting the residuals (i.e., residual = observed measurement - predicted model value).

2. CALIBRATION EXPERIMENTS

The International Atomic Energy Agency's Safeguards Analytical Laboratory (SAL) at Seibersdorf, Austria, has performed calibration experiments to measure the different efficiencies among multi-Faraday detectors. All measurements were made on a Finnigan-MAT 261 mass spectrometer that has nine fixed collectors set up for the isotopes of U from 233 to 238 and for Pu from 238 to 244. The mass spectrometer is controlled by a personal computer running SAL custom-written software. The ionization source utilizes the standard Finnigan-MAT 2 filament geometry, with a Re ionizing filament and a Re evaporation filament. Typical sample loadings are 1 μg of U and 50 ng of Pu. Two types of calibration experiments — peak-shift and peak-jump — were performed to estimate DEFs .

2.1 PEAK-SHIFT EXPERIMENTS

The Finnigan-MAT 261 mass spectrometer has nine Faraday detectors (labeled No. 10 to No. 2) separated by one mass unit (except detector No. 2, which has a two mass unit separation from No. 3). During normal measurements of Pu, detector No. 6 measures isotope ^{239}Pu, and during normal measurements of U, detector No. 8 measures ^{235}U. Different isotopes can be placed into different detectors by moving the mass spectrum to the high- or low-mass side in increments of one mass. This procedure assumes that moving the ion beams will not change significantly the dispersion or the ion incidence angle in the detectors, which would affect the DEFs. In practice, it is only feasible to move the spectrum by 2 masses in either direction. Table 1 illustrates two peak-shift experimental schemes for Pu — each with ten runs that have this restriction. These schemes are not the only ones possible, and Section 4 examines other methods of measurement. Different schemes measure an unequal number of isotopes in each detector. This inequality affects the error limits on the DEFs.

SAL measured four samples labeled 10, 11, 12, and 13 of UK Pu5/92138 [4] to demonstrate peak-shift experiments. Harwell Laboratory prepared the plutonium reference samples to contain plutonium isotopes ^{239}Pu, ^{240}Pu, ^{242}Pu and ^{244}Pu in the approximate ratios of 3:3:3:1. Reported isotopic ratios that are decay corrected to 30 January 1986 with their 95% confidence intervals are: ^{240}Pu/^{239}Pu = 0.9662 (±0.0011), ^{242}Pu/^{239}Pu = 1.0253 (±0.0019) and ^{244}Pu/^{239}Pu = 0.3358 (±0.0008).

SAL measured samples 10 and 11 by peak-shift scheme 1, and samples 12 and 13 by peak-shift scheme 2. The time between runs within each scheme was constant, and the runs were symmetric about the mid-time between runs 5 and 6 (i.e., 5.5). Each sample was measured in three replicates, or blocks, of the ten-run scheme. Time between each block of measurements was used to reset the computer program for the next ten measurements.

Table 1. Plutonium peak-shift experiments for schemes 1 and 2

Scheme 1	Faraday Detectors							No. of
Runs	No. 8	No. 7	No. 6	No. 5	No. 4	No. 3	No. 2	Measure.
1			239	240		242	244	4
2		239	240		242			3
3	239	240		242		244		4
4				239	240			2
5					239	240	242	3
6					239	240	242	3
7				239	240			2
8	239	240		242		244		4
9		239	240		242			3
10			239	240		242	244	4
No. of Measure.	2	4	4	6	6	6	4	32

Scheme 2	Faraday Detectors							No. of
Runs	No. 8	No. 7	No. 6	No. 5	No. 4	No. 3	No. 2	Measure.
1					239	240	242	3
2				239	240			2
3			239	240		242	244	4
4		239	240		242			3
5	240		242		244			3
6	240		242		244			3
7		239	240		242			3
8			239	240		242	244	4
9				239	240			2
10					239	240	242	3
No. of Measure.	2	2	6	4	8	4	4	30

SAL recorded both baseline and ion-signal measurements for each detector. The statistical analysis uses net ion signal (i.e., net ion signal = ion signal - baseline), corrected by a gain-calibration factor, to estimate DEFs and their precision. The net ion signals for detectors measuring the ^{241}Pu position show small but significant values. Most net ion-signal values are less than 1.0 mv (1×10^{-14} A) in absolute value for those detectors not measuring any isotopes of a plutonium sample.

2.2 PEAK-JUMP EXPERIMENTS

Peak-jump experiments select a single isotope to measure ion intensities in each Faraday detector. These measurements are compared to a reference detector. Ion-intensity measurements are first made on a reference detector, then the ion beam is switched to a selected detector. This switching back-and-forth is repeated a number of times until another detector is selected. Figure 1 shows the peak-jump experimental design. SAL performed peak-jump experiments on two samples for each of the three elemental isotopes ^{239}Pu ^{187}Re, and ^{238}U. For example, a sample of ^{239}Pu was first measured in reference detector No. 6 then twice in detector No. 10 then back to detector No. 6 (No. 6, No. 10, No. 10, No. 6). This sequence was followed by the sequence (No. 10, No. 6, No. 6, No. 10). These sequences of 4 runs were repeated for 6 cycles for a total of 24 measurements. The time delays between measurements in different detectors were 8 s and between measurements in the same detector were 2.5 s.

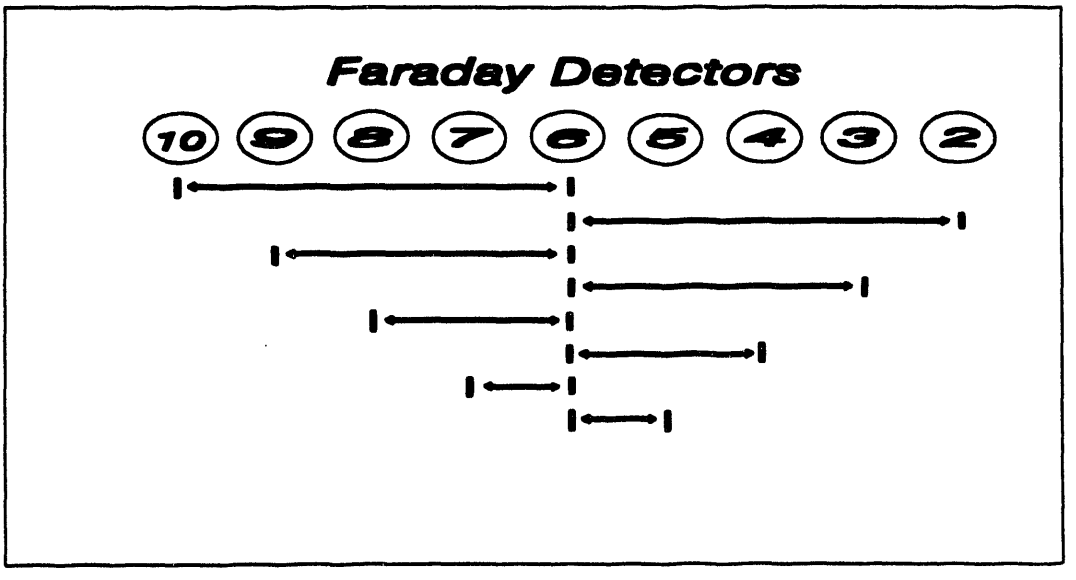

Fig. 1. Measurement scheme for peak-jump experiments.

Advantages of peak-jump experiments are (1) no fractionation is involved for a single isotope, (2) there is no dependency on different isotopes, (3) there is a direct comparison between detectors, (4) they are applicable to any detector configuration, (5) the same magnitude of ion intensities is measured in each detector, and (6) peak-jump experiments are easily performed. Disadvantages of peak-jump experiments are (1) they depend on the element being measured, (2) they involve larger shifts in mass (magnetic field) compared to peak-shift experiments, and (3) they require more experimental time than peak-shift experiments.

3. CALIBRATION MODEL

A flexible calibration model was developed to represent net ion-intensity measurements for both peak-shift and peak-jump experiments. Independent factors in this calibration model account for the major sources of variation that influence the measurement of net ion intensities. These major variation sources are different isotopic masses, different experimental runs (i.e., differences in time) and different Faraday detectors. Other sources of variation that are unknown and cannot be identified are attributed to random variations that are represented by experimental errors. Experimental errors should have a relatively small variance, and an estimate of this variance can be used to judge the adequacy of the fitted calibration model. The variance of the experimental errors is also used to establish uncertainty limits on the calculated DEFs.

A net ion-intensity measurement, Y, can be represented by a function of the sources of variation and experimental error (ε):

$$Y = F(Mass, Run, Detector, \varepsilon). \quad (1)$$

A major problem with approximating the net ion-intensity measurements is to account for the interaction among the sources of variation. For example, if the net ion intensities for each isotopic mass are considerably different, the DEF of an individual detector may change with the magnitude of the ion-intensity values. The rate of change between measurement runs may also depend on the magnitude of the ion intensities. Although some of these interactions can be modeled, Fiedler and Donohue [1] have suggested using samples with relatively equal isotopic ratios to minimize interaction effects.

Detector efficiency factors are ratios relative to a selected detector. These DEFs are used to adjust net ion-intensity measurements relative to the selected or reference detector. Any detector may be selected as the reference detector (in the Results and discussion section, we see that the standard deviations of DEFs depend on the selected reference detector). Detector No. 6 was selected as the reference detector to compare the results of peak-shift experiments with the results of peak-jump experiments.

The experimental-error variance for net ion-intensity measurements is assumed to be proportional to the magnitude of the true net ion-intensity values. As the magnitude of net ion intensities increases, the magnitude of experimental-error variance increases, but the relative error of the measurements is constant. This assumption is equivalent to the condition that the net ion intensities have equal variances on a logarithm scale [5]. Considering this model assumption, the calibration model is formulated as a multiple of exponential functions of the experimental factors

$$Y = K \exp(Mass) \exp[g(Run)] \exp(Detector) \varepsilon, \quad (2)$$

where

K = a multiplying constant.

g(*Run*) = a continuous function of run time. Usually this decay function is assumed to be a linear decreasing function. Additional decay functions will be examined in the fitting process to account for effects due to fractionation and to nonlinear behavior.

exp(*Mass*) = the effect of the isotopic mass. Note, if M_m and M_h are two different isotopes, the isotopic ratio of M_m relative to M_h is $\exp(M_m - M_h)$. This factor is used for peak-shift experiments but not peak-jump experiments that only use single elemental isotopes.

exp(*Detector*) = the effect of the Faraday detector. The DEF for detector D_d relative to detector D_h is $\exp(D_d - D_h)$.

ε = the experimental error. For establishing error limits and testing significance, we assume the errors have a log-normal probability distribution. This assumption means that the logarithms of the errors have a normal probability distribution. In addition, normal errors are assumed to be symmetric about zero with a constant variance. Experimental errors are also assumed to be independent, that is, an error for one measurement is not influenced by an error from another measurement.

For the peak-shift experiment, all factors in the calibration model are estimated. For the peak-jump experiment, factors for isotopic masses [i.e., exp(Mass)] are constant because only a single elemental isotope is measured in each experimental run. Two methods can be used to estimate the parameters in Eq. (2). Nonlinear least squares can be used to estimate the parameters by an iterative method that is computationally intense. However, modern computers make this a minor drawback. A more important limitation is that the estimation of error limits is only approximate. A second method uses the fact that the calibration model is intrinsically linear. This means the calibration model can be linearized by taking logarithms (base e) of both sides of the equation. The parameters in the linearized calibration model can then be estimated by the ordinary method of linear least squares. This standard approach gives us direct methods for calculating error limits and for testing significance differences among model parameters. For

example, the linear calibration model for a net ion-intensity measurement for the *m-th* plutonium isotopic mass, at the *r-th* run time, in the *d-th* detector is

$$\ln(Y_{mrd}) = \ln(K) + M_m + g(R_r) + D_d + \delta_{mrd}, \quad (3)$$

with m = 1, 2, 3, 4; r = 1, 2, ..., 10; and d = 2, 3, ..., 8. The logarithms of the experimental errors (δ_{mrd}) are assumed to be independent random variables and identically distributed as a normal probability distribution with zero mean and a constant variance. Calibration model parameters and their standard deviations are estimated by an analysis-of-covariance model [3], computed by PROC GLM in the SAS computer program [6].

Detector efficiency factors are estimated from net ion-intensity measurements on a sample by using the calibration model in Eq. (3). Initially, the statistical analysis selects a decay function that best represents net ion-intensity change with run time. Next, the calculated isotopic ratios are compared with certified reference values for a validity check on the mass spectrometric analysis of the sample. Finally, the detector efficiency factors are estimated and their uncertainties calculated.

3.1 DECAY FUNCTION g(Run)

The decay function represents the change in net ion intensities as a function of run time. Initially, linear decay functions with a constant slope for each isotope [i.e., g(Run) = βR, R = run time] were fitted to the peak-shift experimental data, and quadratic decay functions [i.e., g(Run) = $\beta R + \gamma R^2$] were fitted to the peak-jump experimental data. For peak-shift experiments, a decay function with different slopes for each isotope can be used to detect fractionation. Comparison of decay functions with different slopes to those with constant slopes indicated no detectable fractionation.

Inadequacies of fitting selected decay functions were examined by plotting the residuals (i.e., residual = observed measurement - predicted measurement). These residuals were scaled [e.g., studentized residuals, (*2*)] so that 99% of the values should fall between –3 and +3. An examination of these residual plots shows that the ion intensities occasionally skip like a step function for both types of calibration experiments. Figure 2 shows a single skip for the peak-shift measurements of plutonium sample = 12-2 (i.e., sample 12 in replicate block = 2). No patterns or physical causes, such as resistance changes in filament contacts, for these skips have been identified. Figure 2 shows the studentized residuals decrease from runs 1 to 5, when a skip occurs between runs 5 and 6, followed by another decrease. Some sample and block studentized residual patterns indicate as many as three skips in the signal response. This decay behavior can be approximated by using a different linear decay function for each set of signal responses where no skips occur [i.e., g(R) = $\alpha + \beta_\alpha R$, where α indicates different skip intervals].

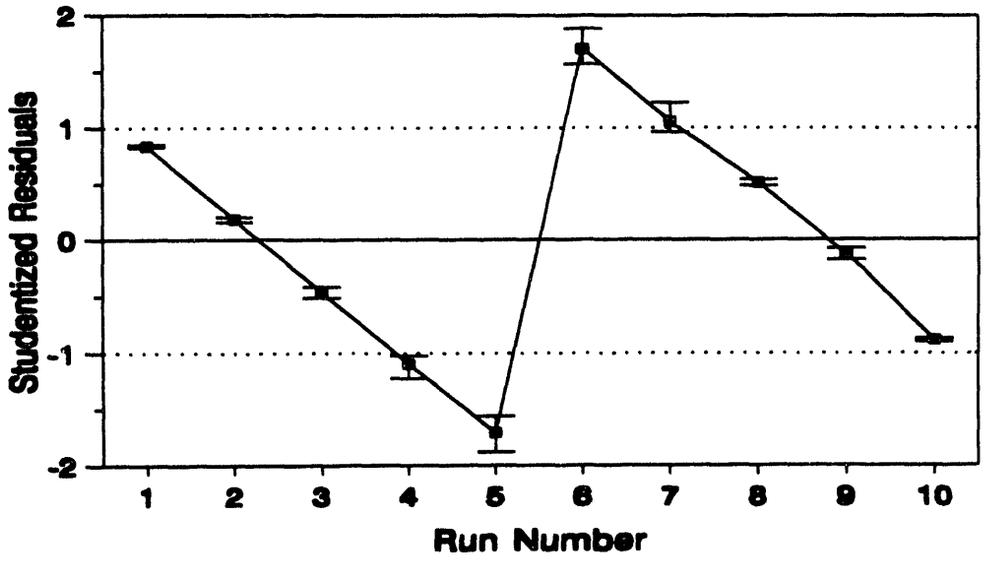

Fig. 2. The ranges of studentized residuals for peak-shift runs on plutonium sample =12-2.

Table 2 shows the changes in estimated standard deviations for experimental errors using either a single linear decay function for each peak-jump experiment or several linear decay functions, depending on the number of skips in an experiment. A good fit of the calibration model to the logarithms of the ion-intensity measurements should have an estimated standard deviation less than 10×10^{-4}. This absolute standard deviation for the log-model in Eq. (3) represents for the calibration model in Eq. (2) a percent relative error [%RE = 100% × (St. Dev of Eq. (2)/(Mean of Eq. (2)] of %RE = 0.1%. These precision measurements are approximately the precisions for fitting the calibration model to background counts in the peak-shift experiments.

Table 2. Estimated standard deviations (x 10^{-4}) for peak-shift experimental errors with corresponding error degrees of freedom in parentheses

Decay	Table 2 shows the changes in estimated standard deviations for experimental errors using Sample-Block											
function*	10-1	10-2	10-3	11-1	11-2	11-3	12-1	12-2	12-3	13-1	13-2	13-3
βR	9.2	21.1	4.3	13.3	15.3	11.2	18.8	102.6	4.2	14.3	16.7	49.4
	(21)	(21)	(21)	(21)	(21)	(21)	(19)	(19)	(19)	(19)	(19)	(19)
$\alpha + \beta_\alpha R$	2.6	1.9	2.4	1.9	2.3	1.2	7.3	4.7	1.1	2.3	2.0	2.5
	(17)	(15)	(17)	(15)	(15)	(15)	(15)	(17)	(13)	(13)	(13)	(13)

*The index α represents different sets of linear signal decay.

Studentized residuals for peak-jump experiments showed skips in eight cases. Figure 3 shows studentized residuals for the first plutonium peak-jump experiment that compares detector No. 7 with reference detector No. 6 (i.e., 7:6). This figure indicates there are two skips. One skip occurs at about 50 s and another occurs at about 115 s.

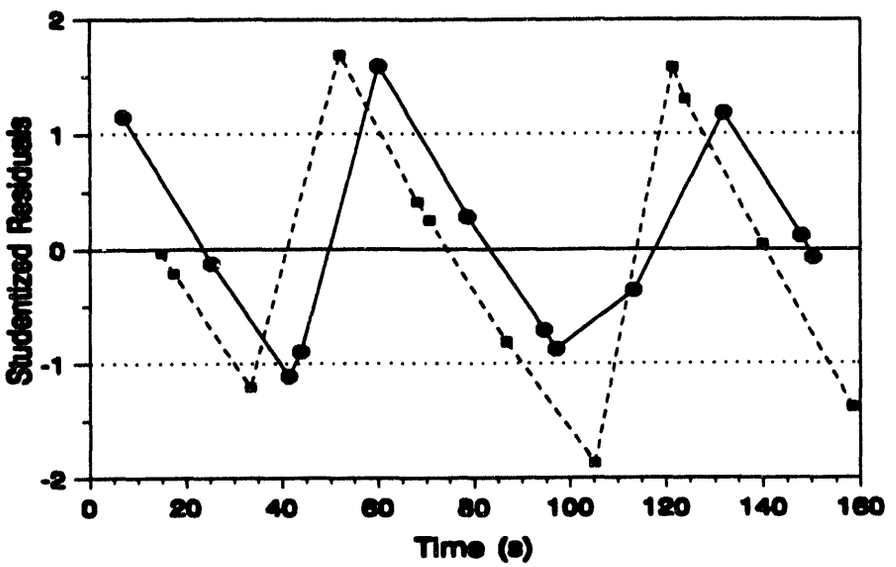

Fig. 3. Studentized residuals for the first ^{239}Pu sample in the peak-jump experiment comparing detector No. 7 (■, square) with detector No. 6 (•, solid circle).

The calibration model can be adjusted for these skips by using a different quadratic decay function for each set of signal responses where no skips occur [i.e., $g(R) = \alpha + \beta_\alpha R + \gamma_\alpha R^2$, where α indicates different skip intervals]. These adjustments for the skip intervals provide good fits to the peak-jump data with estimated standard deviations for experimental errors that are less than 10×10^{-4}. The calibration model in Eq. (3), used to fit both the peak-shift and the peak-jump data, gives equivalent standard deviations for the experimental errors.

3.2 ESTIMATED ISOTOPIC RATIOS

Another evaluation criteria for the peak-shift experiments is the comparison of isotopic ratio estimates to those reported by Harwell Laboratory. Isotopic ratios of UK/Pu5/92138 are estimated from the mass factor [i.e., $\exp(M_m - M_h)$] in the calibration model. The isotopic ratios from three blocks of measurements for a sample should be consistent. The isotopic ratios may not have the same value as the standard reference material because the ion-intensity measurements are not fractionation bias corrected. Figure 4 shows the 12 estimated isotopic ratios for $^{240}Pu/^{239}Pu$. The isotopic ratio estimated for sample 13-3 is larger than other isotopic ratios. Similar results occur for estimates of $^{242}Pu/^{239}Pu$, and $^{244}Pu/^{239}Pu$

isotopic ratios. These larger isotopic ratios in sample 13-3 may indicate a sample preparation problem or an emission anomaly during measurements. The width of the 95% confidence limits for all the isotopic ratios in every sample and block are about the same width as those for the certified values. The combined estimate of the isotopic ratios with their 95% confidence intervals for the four samples with results for sample 13-3 omitted are the following: $^{240}Pu/^{239}Pu$ = 0.9644 (±0.0002), $^{242}Pu/^{239}Pu$ = 1.0248 (±0.0005), and $^{244}Pu/^{239}Pu$ = 0.3354 (±0.0002).

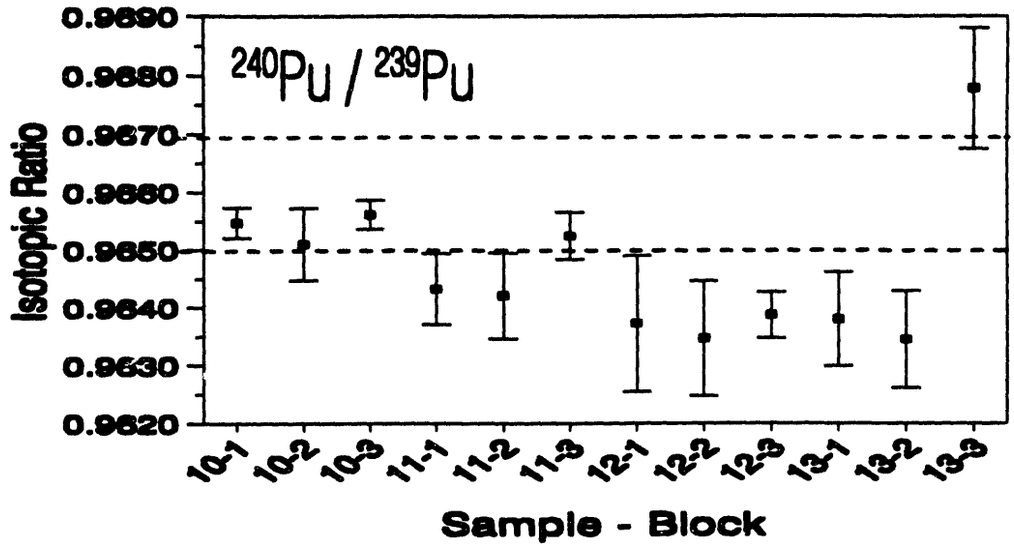

Fig. 4. Plutonium isotopic ratios $^{240}Pu/^{239}Pu$ with their 95% confidence intervals estimated from peak-shift experiments. Dash lines (---) represent lower and upper 95% confidence intervals reported for the UK/Pu5/92138 reference material.

3.3 DETECTOR EFFICIENCY FACTORS (DEFs)

Detector efficiency factors for detector "d" relative to detector "h" are estimated from the detector factors [i.e., $\exp(D_d - D_h)$] in the calibration model. For peak-shift experiments, DEFs are estimated after the data have been adjusted for different masses, linear decay functions, and skips. For the peak-jump experiments, DEFs are estimated after the data are adjusted for quadratic decay functions and skips.

Figure 5 shows the DEFs estimated for the peak-shift experiments. This plot shows that the magnitudes of the DEFs for most sample-block data are ordered as 2:6 ≥ 3:6 ≥ 4:6 ≥ 5:6 ≥ 7:6 ≥ 8:6 except for the DEFs from sample = 13-3. For sample 13-3, the order of the DEF magnitudes is reversed. In addition, there is a much larger spread of DEF values in sample 13-3. The estimated DEFs for sample = 13-3 were not included in the final overall estimates of the DEFs because of the unusual behavior of the estimates for both the isotopic ratios and the DEFs.

Figure 5 also shows large differences among DEF values for sample = 11-1 and 11-2. Also, there is a general increase in the differences for the DEF values from 11-3 to 13-2.

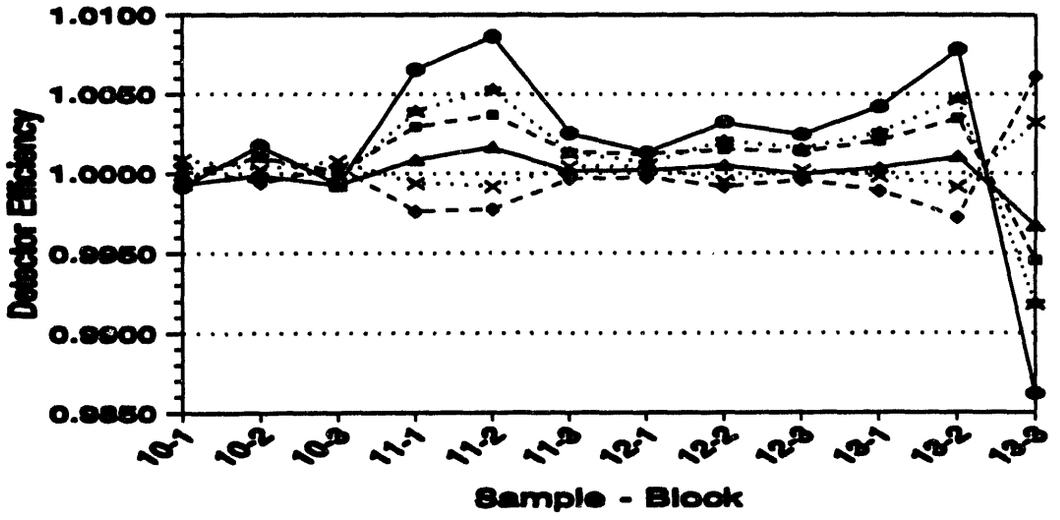

Fig. 5. Detector efficiency factors estimated using peak-shift experiments. Detector ratios are 2:6 (•, circle), 3:6 (★, star), 4:6 (■, square), 5:6 (Δ, triangle), 7:6 (x), and 8:6 (♦, diamond).

Figure 6 shows estimated DEFs from the peak-jump experiments for both replicate samples of the three isotopes (i.e., ^{239}Pu, ^{187}Re, and ^{238}U). Estimated DEFs are reproducible for the rhenium and plutonium replicate experiments. Rhenium DEFs are always larger than plutonium DEFs and uranium DEFs. This result implies that DEF values may depend on either the element or the magnitude of the ion intensities (e.g., 5pA for ^{187}Re vs 40pA for ^{239}Pu and ^{238}U) associated with each sample. Dips are apparent in the DEF values for the ratio 5:6 for all three elements. These dips may be related to the fact that these measurements were the last ones made and the samples were more depleted. Uranium DEFs vary substantially for the different peak-jump experimental runs. Two uranium experimental runs (i.e., ratio 2:6 for run 1, and ratio 5:6 for run 2) have been omitted from the elemental estimates of uranium DEFs. Uranium DEFs for ratio 5:6 in experiment 2 could not be estimated because the ion intensities were lower than the background.

The uranium DEF value (0.9873) for ratio 2:6 in run 1 was unusually low. An inspection of the studentized residuals in Fig. 7 shows that a skip in the net ion intensities occurred in both detectors. Further investigation indicated that both skips were due to increases in net ion intensities, but the increase for detector No. 2 was larger than the increase for detector No. 6.

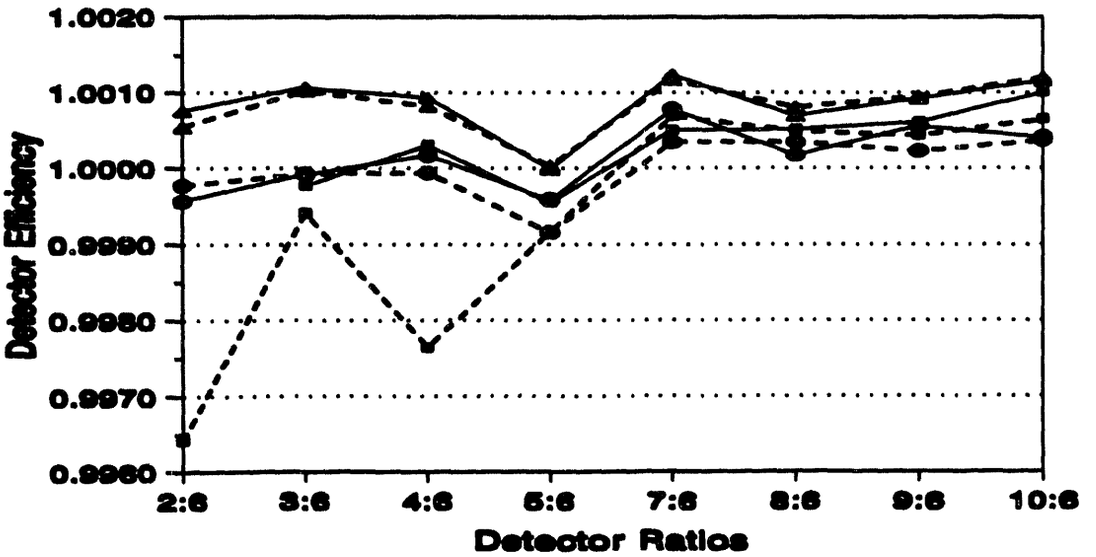

Fig. 6. DEF values for ^{239}Pu (●, circle), ^{187}Re (▲, triangle) and ^{238}U (■, square) using peak-jump experiments. Solid lines represent the first sample, and dash lines represent the second sample.

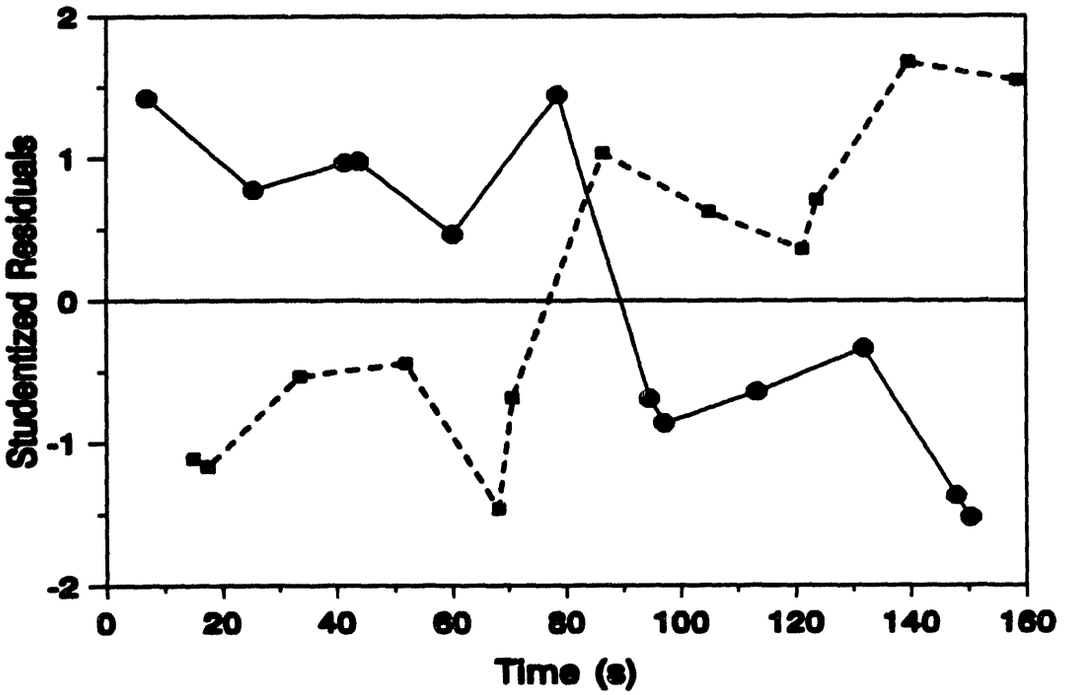

Fig. 7. Studentized residuals for the first ^{238}U sample in the peak-jump experiment comparing detector No. 2 (■, square) with detector No. 6 (●, circle).

Variances for the DEFs from each multidetector calibration experiment can be estimated directly from the method of least squares [2,3]. Combining these variance estimates, confidence intervals can be calculated for the DEFs for each element measured in the multidetector calibration experiments. Table 3 shows the estimated DEFs and their 95% confidence interval estimated from samples of the three elements: plutonium, rhenium, and uranium. The 95% confidence interval on the DEF values for the combined experiments are small, ranging from ±0.0002 to ±0.0010. These confidence intervals for a specific DEF (e.g., 2:6) don't necessarily overlap for peak-shift and peak-jump experiments or for different elements. These results indicate that DEF values are sensitive to the experimental conditions (e.g., temperature fluctuations, signals stability, etc.) and to the type of sample analyzed.

Table 3. DEF estimates and 95% confidence intervals for each element in the multidetector calibration experiments

	Peak-Shift	Peak-Jump		
DEF	Plutonium[a]	Plutonium	Rhenium	Uranium
2:6	1.0034 ± 0.0008	0.9997 ± 0.0006	1.0007± 0.0003	0.9964 ± 0.0010[b]
3:6	1.0020 ± 0.0005	0.9999 ± 0.0006	1.0010 ± 0.0009	0.9996 ± 0.0010
4:6	1.0017 ± 0.0003	1.0001 ± 0.0007	1.0009 ± 0.0006	0.9990 ± 0.0005
5:6	1.0003 ± 0.0002	0.9994 ± 0.0010	1.0000 ± 0.0003	0.9996 ± 0.0008[c]
7:6	1.0000 ± 0.0003	1.0006 ± 0.0010	1.0012 ± 0.0005	1.0006 ± 0.0009
8:6	0.9991 ± 0.0003	1.0003 ± 0.0005	1.0008 ± 0.0002	1.0005 ± 0.0008
9:6		1.0004 ± 0.0007	1.0009 ± 0.0002	1.0005 ± 0.0010
10:6		1.0004 ± 0.0009	1.0012 ± 0.0002	1.0008 ± 0.0009

[a]Omitted results from peak-shift experiment for sample = 13-3.
[b]Omitted results from first uranium peak-jump experiment for DEF = 2:6.
[c]Omitted results from second uranium peak-jump experiment for DEF = 5:6.

4. PEAK-SHIFT EXPERIMENTAL DESIGNS

Faraday detectors No. 6, No. 5, No. 3, and No. 2 measure ^{239}Pu, ^{240}Pu, ^{242}Pu, and ^{244}Pu, respectively, during the normal operation of mass spectrometric analyses. Two peak-shift experimental designs labeled scheme 1 and scheme 2 were used to estimate DEFs for the four detectors. Both schemes can be used to estimate DEFs, but the variances of the estimated DEFs depend on the chosen scheme. Comparisons of the two schemes will be made by examining their effect on the precision of the estimated DEFs.

A DEF (say, D_j relative to D_k) is estimated by $\exp(D_j - D_k)$. For the calibration model in Eq. (3), this DEF estimate is equivalent to the difference between the two detector effects. The variance of this difference can be calculated from the individual variances and their covariance by [3]

$$Var(D_j - D_k) = Var(D_j) + Var(D_k) - 2\,Cov(D_j, D_k) \quad , \quad (4)$$

$$Var(D_j - D_k) = a_{jj}\sigma^2 + a_{kk}\sigma^2 - 2a_{jk}\sigma^2 = h(X)\sigma^2 \; . \quad (5)$$

The variance of a DEF is a product of two numbers, a design multiplying factor and a variance factor. The variance factor (σ^2) depends only on the variation of the mass spectrometric measurements. The design multiplying factor h(**X**) is a weighting factor that doesn't depend on any measurement data but only on the peak-shift calibration experiment (**X**) and the calibration model. Values of h(**X**) are calculated from the variance-covariance matrix [3] by using the elements corresponding to the variance of the two detectors (a_{jj} and a_{kk}) and to the covariance between the two detector (a_{jk}). Different peak-shift experiments can be compared for estimating a DEF by examining the associated h(**X**) values for the same calibration model. The smallest variance for an estimated DEF would correspond to the peak-shift experiment with the smallest h(**X**) value.

Each DEF has a different h(**X**) value for a peak-shift experiment. The average h(**X**) over those DEFs used in the normal operating mode represents an overall precision measure of DEFs associated with a peak-shift experiment. Table 4 shows h(**X**) values corresponding to DEFs 2:6, 3:6, and 5:6 using peak-shift experiments for schemes 1 and 2. These h(**X**) values are calculated for the calibration model in Eq. (3) using a linear decay function with no skips.

Table 4. Design multiplying factors h(X) for peak-shift experiments using schemes 1 and 2 [a]

Peak-Shift Experiment	Detector Efficiency Factor			
	2:6	3:6	5:6	Average
Scheme 1	0.810	0.571	0.446	0.609
Scheme 2	0.441	0.424	0.441	0.436

[a]The calibration model uses a linear decay function.

The average h(X) value for scheme 2 (0.436) is smaller than the average h(X) value for scheme 1 (0.609). This result indicates that the average variance of the DEFs estimated from scheme 2 would be smaller than average variance of those DEFs estimated from scheme 1 for the same value of σ^2 . Design multiplying factors also depend on which detector is used as the reference detector in the denominator of DEF ratios because the number of measurements is not equal for all detectors.

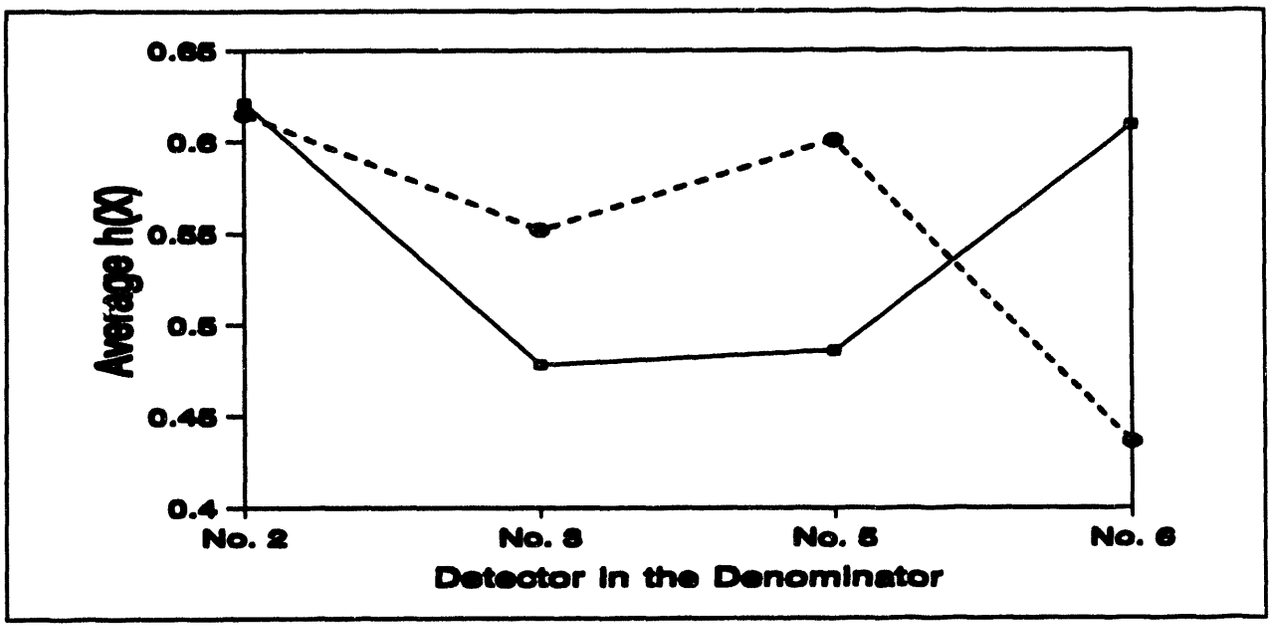

Fig. 8. Average design multiplying factors h(X) for peak-shift experiments using different detectors in the denominator of the DEFs. DEFs for scheme 1 (■, square) and scheme 2 (•, circle) are based on a calibration model with a linear decay function.

Figure 8 shows the average h(**X**) values associated with DEFs with different reference detectors in the denominator. Scheme 2 produces the minimum average h(**X**) value (0.436) for DEFs relative to reference detector No. 6. For DEFs relative to reference detector No. 3, scheme 1 has a smaller average h(**X**) value (0.478) than the h(**X**) value for scheme 2 (0.552). This example shows that the precision of the DEFs depends not only on the type of peak-shift experiment but also on the reference detector used in the denominator of the DEFs.

4.1 BEST PEAK-SHIFT EXPERIMENTS

Peak-shift experimental designs for estimating DEFs should have the following properties:

1. The peak-shift experiment should estimate the DEFs that are relative to a detector used for the normal operating mode (e.g., No. 2, No. 3, No. 5, and No. 6 for plutonium). A minimum number of runs is required to estimate all the calibration model parameters.

2. The peak-shift experiment should have the most isotopic measurements in the detectors used in the normal operating mode.

3. A peak-shift experiment with properties 1 and 2 is an optimal DEF peak-shift experiment if it has the smallest average design multiplying factor for those DEFs associated with the normal operating mode.

Table 5 shows the ten possible measurements for plutonium that can be made in a peak-shift experiment. The rows (3 through 8) are identified by letters (A through F), with the number of isotopes being measured in detector Nos. 2 through 6 in parentheses. Rows 1, 2, 9, and 10 can be eliminated from consideration because they provide only a single measurement in detector Nos. 2 through 6. Row 5, identified by C(4), is the normal operating position, which contributes four isotopic measurements in detector Nos. 2 through 6. Row 3, identified by A(3), provides the next largest number of isotopes in detector Nos. 2 through 6. The seven measurements from the combined rows of C(4) + A(3) cannot estimate all DEFs. An additional row must be selected from rows B(2), D(2), E(2), and F(2) to estimate all DEFs. Any of the four designs A+C+B, A+C+D, A+C+E, and A+C+F can estimate the DEFs. These peak-shift experiments were checked for the estimability [3] of the DEFs by using a calibration model in Eq. (3) with no decay function.

Table 5. Possible measurements for peak-shift experiments. Measurements in bold-type (row 5) represent mass spectrometric analyses during normal operation

	Faraday Detectors									
Row	No. 10	No. 9	No. 8	No. 7	No. 6	No. 5	No. 4	No. 3	No. 2	ID
1									239	
2								239		
3							239	240	242	A(3)
4						239	240			B(2)
5					**239**	**240**		**242**	**244**	C(4)
6				239	240		242			D(2)
7			239	240		242		244		E(2)
8		239	240		242		244			F(2)
9	239	240		242		244				
10	240		242		244					

Peak-shift experiment (A,C,D) has the smallest average h(X) (1.667) for DEFs relative to detector No. 3. This calibration experiment requires the fewest runs for a peak-shift experiment that can be used for a multidetector calibration experiment for plutonium. The best peak-shift experiment with four rows started with the best peak-shift experiment with three rows (A,C,D) and added another row from rows A, B, C, D, E, and F. The best four-row peak-shift experiment is (A,C,D,E), with an average h(X) of 1.020 for DEFs relative to detector No. 3.

Similarly, the best peak-shift experiment with five rows was found by adding a row to the best four-row peak-shift experiment. The best peak-shift experiment with five rows is (A,C,D,E, F), with an average h(X) value of 0.761 for DEFs relative to detector No. 6. Peak-shift experiments using scheme 1 duplicate the five rows (C,D,E,B,A). This five-row peak-shift experiment has an average h(X) of 0.956 for DEFs relative to detector No. 3.

A peak-shift experiment using scheme 2 replicate the five rows (A,B,C,D,F), with an average h(X) of 0.871 relative to detector No. 6, which was not examined by this design selection method. Scheme 2 illustrates that the searching method for good peak-shift experiments does not examine all possible combinations (6^5 = 7776) of the six possible rows. This limited search method constructs good experiments even if they must be terminated early. For example, if a chemist plans to do a five-run experiment, but the last two runs have invalid results, then the first three runs still make a good peak-shift experiment (A,C,D).

The best ten-row peak-shift experiment was constructed by duplicating the best five-row peak-shift experiment. Table 6 compares this best peak-shift experiment with peak-shift experiments for schemes 1 and 2 using a constant decay function [$g(R_r)$ = constant], a linear decay function [$g(R_r) = \beta R_r$], and a quadratic decay function [$g(R_r) = \beta R_r + \gamma R^2$]. For the linear decay function, the rows of the best peak-shift experiment were symmetrically ordered about the middle rows. The rows were ordered so that the largest number of measurements in detector Nos. 2 and 6 are in the first and last experimental rows [i.e., C(4), A(3), D(2), E(2), F(2), F(2), E(2), D(2), A(3), C(4)].

Table 6. Average design multiplying factors for calibration models with either a constant, a linear or a quadratic decay function

Decay Function	Peak-Shift Experiment	Faraday Detector in the Denominator of the DEFs			
		No. 2	No. 3	No. 5	No. 6
No Decay	Best	0.529	0.426	0.498	0.454
	Scheme 1	0.621	0.478	0.486	0.609
	Scheme 2	0.615	0.552	0.601	0.436
Linear	Best	0.486	0.399	0.482	0.381
	Scheme 1	0.621	0.478	0.486	0.609
	Scheme 2	0.615	0.552	0.601	0.436
Quadratic	Best	0.666	0.455	0.544	0.529
	Scheme 1	0.683	0.528	0.519	0.726
	Scheme 2	1.166	0.817	0.940	0.861

Table 6 shows that the average h(**X**) values are the same for peak-shift experiments using both scheme 1 and scheme 2 for either a constant decay function or a linear decay function. For quadratic decay functions, these average h(**X**) are different. For the three decay functions, the best peak-shift experiment gives the lowest average h(**X**) value and would be the peak-shift experiment of choice for multidetector calibration experiments.

4.2 ESTIMATING PLUTONIUM ISOTOPIC RATIOS FROM THREE RUNS

In Sect. 4.1, we determined that the best three-run calibration experiment was the one with rows (A,C,D) in Table 5. This minimum peak-shift experiment can be used to estimate isotopic ratios that are adjusted for variations among the different detectors. In addition, a three-run measurement sample analysis would minimize the influence of fractionation because of the reduced measurement time.

The purpose of using a minimum peak-shift experiment for a sample analysis is to adjust the estimated isotopic ratios for DEFs during each sample analysis rather than estimating overall DEFs for all sample runs in a calibration experiment. For a peak-shift sample analysis, the chemist would assume that the decay function, $g(R_r)$, is constant over the three runs. The linear model in Eq. (3) for a plutonium sample analysis would be

$$Z_{m,d} = \ln(Y_{md}) = \ln(K) + M_m + D_d + \delta_{md} , \qquad (6)$$

with index m = 9, 0, 2, 4 for ^{239}Pu, ^{240}Pu, ^{242}Pu, and ^{244}Pu, respectively. The index d = 7, 6, 5, 4, 3, and 2 for the corresponding detectors. No index for rows (i.e., r) is needed because the decay function is assumed to be constant. Table 7 shows the three-run peak-shift measurements of the logarithm of the ion-intensities.

Table 7. Logarithm measurements from a three-run peak-shift sample analysis

Run	Faraday Detectors						ID
	No. 7	No. 6	No. 5	No. 4	No. 3	No. 2	
1				$Z_{9,4}$	$Z_{0,3}$	$Z_{2,2}$	A(3)
2		$Z_{9,6}$	$Z_{0,5}$		$Z_{2,3}$	$Z_{4,2}$	C(4)
3	$Z_{9,7}$	$Z_{0,6}$		$Z_{2,4}$			D(2)

Isotopic ratios relative to ^{239}Pu are estimated by $\exp(M_m - M_9)$, for m = 0, 2, 4. A least-squares analysis [5] of the data in Table 7 will give estimates of the differences between the mass effects. These estimates are based on summing the Z-values in Table 7 either over each mass or over each detector. A "dot" notation in the index will represent sums over all Z-values for the specified index. For example, the sum over all detectors for mass = 239 is
and the sum over all masses for detector 2 is

$$Z_{9,.} = Z_{9,4} + Z_{9,6} + Z_{9,7} , \qquad (7)$$

$$Z_{.,2} = Z_{2,2} + Z_{4,2} \quad . \tag{8}$$

The sum $Z_{..}$ represents the total sum of the measurements in Table 7.

The estimated differences (e.g., M_m - M_9) are a linear combination of sums on the Z-values

$$M_0 - M_9 = \frac{1}{3}\left[2Z_{.,.} - 2Z_{9,.} + 2Z_{0,.} - 2Z_{.,2} - 3Z_{.,3} - Z_{.,4} - 4Z_{.,5} - 2Z_{.,6}\right] , \tag{9}$$

$$M_2 - M_9 = \frac{1}{3}\left[4Z_{.,.} - 4Z_{9,.} - 2Z_{0,.} - 4Z_{.,2} - 3Z_{.,3} - 2Z_{.,4} - 2Z_{.,5} - Z_{.,6}\right] , \tag{10}$$

$$M_4 - M_9 = \frac{1}{3}\left[10Z_{.,.} - 10Z_{9,.} - 8Z_{0,.} - 6Z_{2,.} - 7Z_{.,2} - 3Z_{.,3} - 2Z_{.,4} - 2Z_{.,5} - Z_{.,6}\right] . \tag{11}$$

Example Table 8 summaries a hypothetical data set from three runs of a peak-shift analysis of a plutonium sample. The estimated differences are the following:

$M_0 - M_9 = [\ 2(152) - 2(58) + 2(49) - 2(20) - 3(26) - (30) - 4(17) - 2(38)\ ]/3,$

$M_0 - M_9 = -2,$

$M_2 - M_9 = [\ 4(152) - 4(58) - 2(49) - 4(20) - 3(26) - 2(30) - 2(17) - (38)\ ]/3,$

$M_2 - M_9 = -4,$

$M_4 - M_9 = [\ 10(152) - 10(58) - 8(49) - 6(36) - 7(20) - 3(26) - 2(30) - 2(17) - (38)\ ]/3,$

$M_4 - M_9 = -6.$

Table 8. Hypothetical data from three runs of a peak-shift analysis of a plutonium sample

Mass	Faraday Detectors						Sum
	No. 2	No.3	No. 4	No. 5	No. 6	No. 7	
239			17		20	21	58
240		14		17	18		49
242	11	12	13				36
244	9						9
Sum	20	26	30	17	38	21	152

The data for this example were generated by the model $Z_{m,d} = 10 + M_m + D_d$, with $M_9 = 8$, $M_0 = 6$, $M_2 = 4$, $M_4 = 2$; $D_2 = -3$, $D_3 = -2$, $D_4 = -1$, $D_5 = +1$, $D_6 = +2$, and $D_7 = +3$. No experimental error was added to the hypothetical data in order to simplify the calculations for the example. The example shows that unbiased estimates of the mass effect differences (e.g., $M_m - M_9$) can be obtained to calculate the isotopic ratios [e.g., $\exp(M_m - M_9)$].

Experimental error does contribute to measured ion-intensities during spectrometric analyses of samples. The standard deviation of the mass effect differences can be related to the standard deviation of the Z-values (logarithm of the ion-intensity measurements). These standard deviations are calculated for the three-run (A,C,D) peak-shift analysis by

$$\text{St. Dev. of } (M_{240} - M_{239}) = \frac{2}{\sqrt{3}} \sigma , \qquad (12)$$

$$\text{St. Dev. of } (M_{242} - M_{239}) = \frac{2}{\sqrt{3}} \sigma , \qquad (13)$$

and

$$\text{St. Dev. of } (M_{244} - M_{239}) = \sqrt{\frac{10}{3}} \sigma . \qquad (14)$$

The standard deviation of the Z-values are denoted by σ.

The three-run peak-shift analysis would only have one degree of freedom to estimate the value of σ by the square root of the mean square error from a statistical regression analysis. The standard deviation from many sample analyses ($\geq$20) could be pooled for an overall estimate of the standard deviation of the Z-values. From this well-known estimate, two-sided 95% confidence intervals can be calculated for the isotopic ratios based on the 0.025 percentile point (i.e., 1.96) of the normal distribution. A standard deviation estimate based on a smaller number of sample analyses would use percentiles of a Student's t-distribution.

$$95\%\ \text{C.I.}\ \frac{Pu^{240}}{Pu^{239}} : \exp\left(M_{240} - M_{239} \pm 2.263\,\sigma \right) , \qquad \textbf{(15)}$$

$$95\%\ \text{C.I.}\ \frac{Pu^{242}}{Pu^{239}} : \exp\left(M_{242} - M_{239} \pm 2.263\,\sigma \right) , \qquad \textbf{(16)}$$

and

$$95\%\ \text{C.I.}\ \frac{Pu^{244}}{Pu^{239}} : \exp\left(M_{244} - M_{239} \pm 3.579\,\sigma \right) . \qquad \textbf{(17)}$$

The multipliers of σ in the exponentials are $2.263 = 1.96 \times \frac{2}{\sqrt{3}}$ and $3.579 = 1.96 \times \sqrt{\frac{10}{3}}$.

5. CONCLUSIONS

A flexible calibration model is used to statistically analyze data from both peak-shift and peak-jump experiments using standard linear regression methodology. Analysis of the residuals from the fitted calibration model reveals that skips occur in the ion intensities for both types of calibration experiments. Although the causes for these skips have not been identified, a shift term was added to the decay function to adjust the calibration model.

The DEF values estimated from the peak-shift experiments show a similar ordering of all DEF magnitudes except for sample = 13-3. This ordering indicates the DEF values are proportional to the distance from the reference detector. Residual analysis for sample = 13-3 indicates that the DEF values can reverse the ordering of their magnitudes. For peak-jump experiments, the first uranium sample for the ratio 2:6 demonstrates a non-uniform skip for net ion intensities for the two detectors. Additional investigation is needed to reveal the causes of these anomalies before any DEF values can be recommended to adjust mass spectrometric analyses on unknown samples.

The rhenium DEF values estimated for the peak-jump are all greater than 1. These DEF values are significantly larger than the calculated DEF values for both plutonium and uranium samples. These differences may be due to the magnitude of the net ion intensities measured for each element.

Peak-shift experiments and peak-jump experiments do not give unique DEF values that can be used for all elements or for all replicate mass spectrometric analyses. This variability is a major problem for estimating DEF values. Additional multidetector calibration experiments may be required to detect the underlying causes for inconsistent DEF values.

An investigation of the best peak-shift experiments showed that a minimum of three runs are required to estimate both the isotopic ratios and the detector efficiency factors. This investigation suggests that isotopic ratios be calculated from a three-run peak-shift sample analysis. A statistical analysis of this minimum peak-shift sample analysis can adjust the isotopic ratios for any effects due to different detectors during the sample analysis.

6. REFERENCES

1. R. Fiedler and D. Donohue, "Pocket Sensitivity Calibration of Multicollector Mass Spectrometers," *Fresenius Z. Anal. Chem.*, 331 (1988) 209.

2. N. Draper and H. Smith, *Applied Regression Analysis, Second Edition*, Wiley, New York, 1981, Chapters 2 and 3.

3. S. R. Searle, *Linear Models*. Wiley, New York, 1971, Chapter 5.

4. F. E. Hamilton, A. P. Knight, I. Maidment, A. M. Thomas, and A. J. Wood, *The Preparation and Characterisation of a 3:3:3:1 Mixture of ^{239}Pu:^{240}Pu:^{242}Pu:^{244}Pu for Use as an Isotopic Reference Material for Mass Spectrometric Analysis*, UK Safeguards R&D Project, SRDP-R155, Harwell Laboratory, UK, 1989.

5. J. Aitchison, and J. A. C. Brown, *The Lognormal Distribution*, Cambridge University Press, London, 1976, Chapter 1.

6. SAS Institute, Inc., *SAS/STAT™ Guide for Personal Computers, Version 6.03*, SAS Institute, Inc., Cary, N.C., 1985.

INTERNAL DISTRIBUTION

1. C. M. Barshick
2-6. C. K. Bayne
7. J. N. Cooley
8. D. C. Duckworth
9. D. H. Pike
10-12. C. H. Shappert
13. D. H. Smith
14. G. E. Whitesides
15. Central Research Library
16. ORNL Y-12 Technical Library Document Reference Section
17. Laboratory Records Department
18. Laboratory Records Department, RC
19. ORNL Patent Office

EXTERNAL DISTRIBUTION

Los Alamos National Laboratory, Group CST-1, Mail Stop G-740, Los Alamos, New Mexico 87545

20. J. H. Cappis
21. E. L. Callis

International Atomic Energy Agency, Safeguards Analytical Laboratory, Wagramerstrasse 5, P. O. Box 100, A-1400 Vienna, Austria

22. H. Aigner
23. G. Bagliano
24. D. Donohue
25. S. Deron
26. N. Doubek
27. R. Fiedler
28. J. Parus

International Safeguards Project Office, Building 475B, Brookhaven National Laboratory, Upton, L. I., New York 11973

29-103. Ms. Michele M. Rabatin

104. Office of Deputy Assistant Manager for Energy Research and Development, Department of Energy, Oak Ridge Operations (DOE-ORO) P.O. Box 2008, Oak Ridge, TN 37831-6269.
105-106. Office of Scientific and Technical Information, U.S. Department of Energy, P.O. Box 62, Oak Ridge, TN 37831.

DATE

FILMED

9/9/94

END